UCRL--53198

DE82 005856

DISCLAIMER

As-Built Mechanical and Thermomechanical Calculations of a Spent Fuel Test in Climax Stock Granite

T. R. Butkovich

Manuscript date: September 1981

LAWRENCE LIVERMORE LABORATORY
University of California • Livermore, California • 94550

Available from National Technical Information Service • U. S. Department of Commerce
5285 Port Royal Road • Springfield, VA 22161 • $6.00 per copy • (Microfiche $3.50)

AS-BUILT MECHANICAL AND THERMOMECHANICAL CALCULATIONS OF A SPENT-FUEL TEST IN CLIMAX STOCK GRANITE

ABSTRACT

A generic test of geological storage of spent-fuel assemblies from an operating nuclear reactor in Climax Stock granite has been underway at the U.S. Department of Energy's Nevada Test Site since spring 1980. The spent-fuel assemblies were emplaced in the floor of the central drift of three parallel drifts. The drifts are spaced 10 m on center and lie 420 m (1370 ft) below the surface. Auxiliary electric heaters were installed in the floors of the side drifts to simulate a large repository.

Calculational modeling of the spent-fuel repository was made with the finite element codes, ADINA stress analysis code and the compatible ADINAT heat flow code. The material was assumed to be isotropic-thermoelastic, with a temperature-dependent thermal expansion coefficient. The primary purpose for doing the calculations was to provide results with the best estimates of physical and mechanical rock properties and *in situ* stresses.

Field measurements show the effective modulus of Climax Stock granite is a factor of two lower than that obtained in the laboratory on small samples. Comparative calculations using these field measurements and measurements obtained in the laboratory show displacements are approximately inversely proportional to the modulus. They also indicate the importance of knowing the effective *in situ* modulus. Another comparison, varying the *in situ* stress loading, shows the importance of knowing the correct value of *in situ* stress.

Calculations using the best-estimate values of rock properties, effective *in situ* modulus and Poisson's ratio, and *in situ* stress are not intended to predict the displacement and stress changes from the mining and the imposition of a thermal load. The existing jointing in the Climax Stock granite could have a significant effect on the actual displacements and stress field. Such effects are not accounted for here. However, these calculations do indicate the direction and magnitude of displacements and stresses that would be expected in absence of jointing. Comparison of those results with actual field measurements will, thus, indicate the significance of including a joint model in future calculations.

INTRODUCTION

Geological storage of spent-fuel assemblies from an operating nuclear reactor has been underway since the spring of 1980 at the U.S. Department of Energy's Nevada Test Site. The primary objectives of this generic test are: a) evaluating granite as a medium for deep geological storage of high-level reactor waste; and b) providing data on the thermal and thermomechanical behavior of the granite surrounding the excavations. With these data we expect to develop and improve computational tools to model the behavior of any future hard-rock repositories.

Preemplacement calculations were made of the effects of the mining operation and thermal loading on the existing stress fields and resultant displacements of rock around the excavations.[1] The calculations provide a base from which to compare stress and displacement data. These results have already proved useful in comparing and projecting future results. The preemplacement calculations were made with the ADINA[2] structural analysis code and the compatible ADINAT[3] heat-flow code. These finite element codes were chosen because of their ability to handle diverse factors (such as heat flow) by conduction, convection, radiation and ventilation, thermoelasticity, excavation, and a future capability of ubiquitous or discrete joint models. The preemplacement calculations were made using the isotropic-thermoelastic model in ADINA. ADINAT was adapted to model internal radiative heat transport within the drifts and the effects of ventilation.[4]

The preemplacement calculations were made with the expected power level of the spent-fuel canisters calculated using the ORIGEN code.[5] Later calorimetry measurements showed the expected 1.858-kW power level at emplacement time to be about 22% too high.[6] As a result of this, the planned power levels of the electrical simulators and auxiliary heaters were changed.

The preemplacement calculation was made using an elastic modulus based on measurements on small samples of rock taken from the site. Since then, a better understanding of the effective moduli of Climax Stock granite surrounding the excavations has emerged. Field measurements show the effective moduli almost 50% lower than indicated by laboratory measurements.[7] In addition, a region around each opening was damaged by explosives used during excavation. This region was found to have an effective modulus of about a factor of two below that of the surrounding rock.[8]

The U.S. Geological Survey measured the *in situ* state of stress at the site using the United States Bureau of Mines (USBM) overcore technique.[9] These and other measurements were used to calculate ratios of horizontal-to-vertical stress, the highest value being 1.25.[8] The preemplacement calculation assumed both stresses to be isotropic and equal to ρgh.

The ADINA and ADINAT calculations were repeated because of the variety of differences between planned and actual heat loading and better information regarding *in situ* effective moduli and *in situ* stress. The as-built ADINAT calculation used the correct values of heat input and the best available laboratory and field-measured thermal properties of the rock. The as-built *ADINA* calculation used the best estimates of the moduli and loading, based on *in situ* measurements. Furthermore, other ADINA calculations were made to study the sensitivity of varying the moduli and loading on the results for both the mining and thermal portions of the test. All of these calculations were made before displacement or stress-change data were available from the heated phase of the experiment.

LAYOUT OF THE TEST REPOSITORY AND ACQUISITION OF DATA

The underground installation in the Climax Stock granite was excavated at the 420-m (1370-ft) level (Fig. 1). Three drifts, spaced on 10-m centers, were excavated in three steps. The two side drifts were excavated first in a single pass. The center drift was excavated in two passes, first the top heading, then the bench. Following the excavation of the side drifts, multiposition extensometers and stress gauges were emplaced at two stations (Fig. 2) and relative displacements between anchors and sensing heads were measured. Stress data during the mine-by were obtained in one pillar at two stations.

The central drift is used for the storage of the spent-fuel canisters and electrical simulators, while the side drifts contain auxiliary electrical heaters. Seventeen vertical storage holes on 3-m centers were sunk in the floor of the central drift to a depth of 6 m (20 ft). Of these holes, 11 are being used for spent-fuel canister storage and six are being used for thermally-identical electrical simulators. Electrical resistance heaters have been emplaced in vertical holes on 6-m centers in the floors of the side drifts.

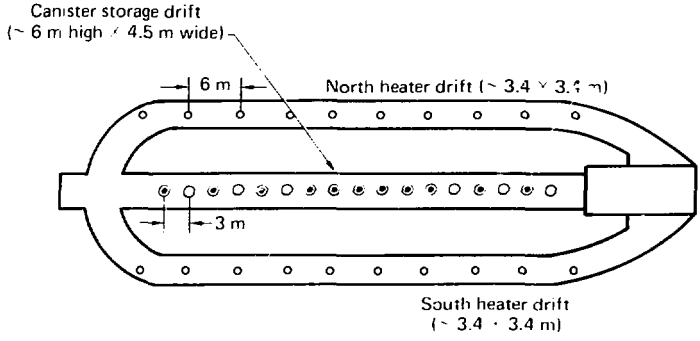

FIG. 1. Layout of the drifts and positions of the spent-fuel canisters, electrical simulators and electrical heaters.

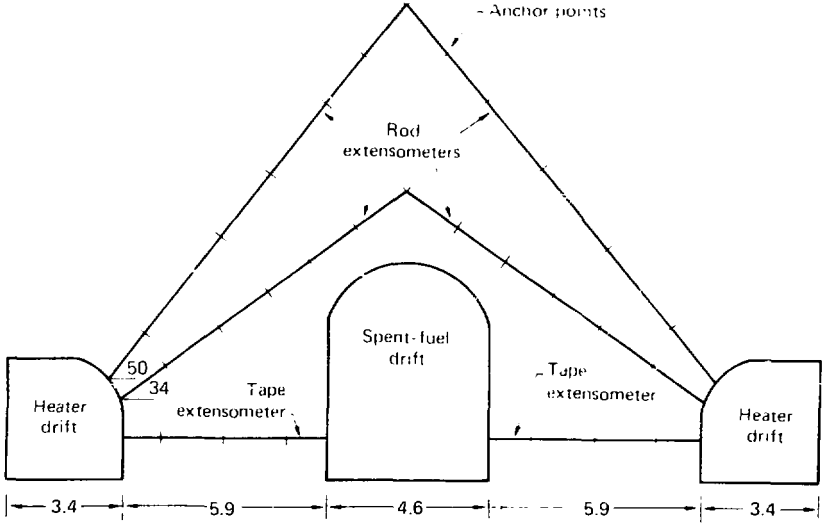

FIG. 2. Layout of one of two extensometer stations, shown in a schematic elevation view through the spent-fuel (central) and heater (side) drifts. The tick marks represent anchor points, to which relative displacements are being measured with respect to hole collars at the walls of the side drifts. Dimensions are in metres.

The thermal ouput of these heaters will be periodically adjusted to simulate the thermal regime of a large storage array.

Rock temperatures, stresses, and displacements in the central region around the canister drift are being measured continually during the planned 3- to 5-yr storage period, and data will be compared with the calculated results in future reports. Instrumentation that has been distributed throughout the test repository includes nearly 500 thermocouples for measuring temperatures; 26 extensometers with 116 anchor points, and 34 convergence wire heads with attachment fixtures for tape extensometers to measure relative displacements; 21 transducers for monitoring fracture motion; and 18 stress gauges. Of the instrumentation installed for the mine-by experiment, only the stress gauges were removed. The mine-by extensometers are included in the inventory given above.

CALCULATIONAL INPUT

As with the preemplacement calculations, the as-built calculations are two-dimensional, and the geometry of the drifts in both sets is identical and based on as-built dimensions. Table 1 shows the distances and spacings used in the construction of the finite-element mesh.

TABLE 1. Distances and dimensions used in ADINA and ADINAT calculations.

	Distances and dimensions
Spent-fuel drift	
Floor position	417.58 m below surface 1.75 m above top of canister
Cross section	4.58 × 6.25-m domed roof
Heater drift	
Floor position	417.58 m below surface 2.66 m above top of heater
Cross section	3.35 × 3.35-m rounded corner
Spent-fuel canisters and electrical simulators	
Spacing	3 m on center
Length	3.66 m
Electrical resistance heaters	
Spacing	6 m on center
Length	1.83 m

The finite-element mesh used in the as-built calculations reported here was redesigned to allow for an element group 0.5 m wide surrounding the excavations so that a rock zone damaged by explosive shock during the excavations could be treated differently from the rest of the rock. Figure 3(a) shows the entire mesh and Fig. 3(b) shows a close-up view of the same mesh illustrating the 0.5-m-wide zone. All of the elements consist of eight nodes, with the exception of degenerated four-node elements used to represent the material removed during the excavation.

Table 2 shows the thermal properties used in both the preemplacement and the current as-built calculations. Of the Climax Stock granite properties, the thermal conductivities are taken from averages in Ref. 10 that have been normalized to *in situ* measurements obtained during the heater test.[11]

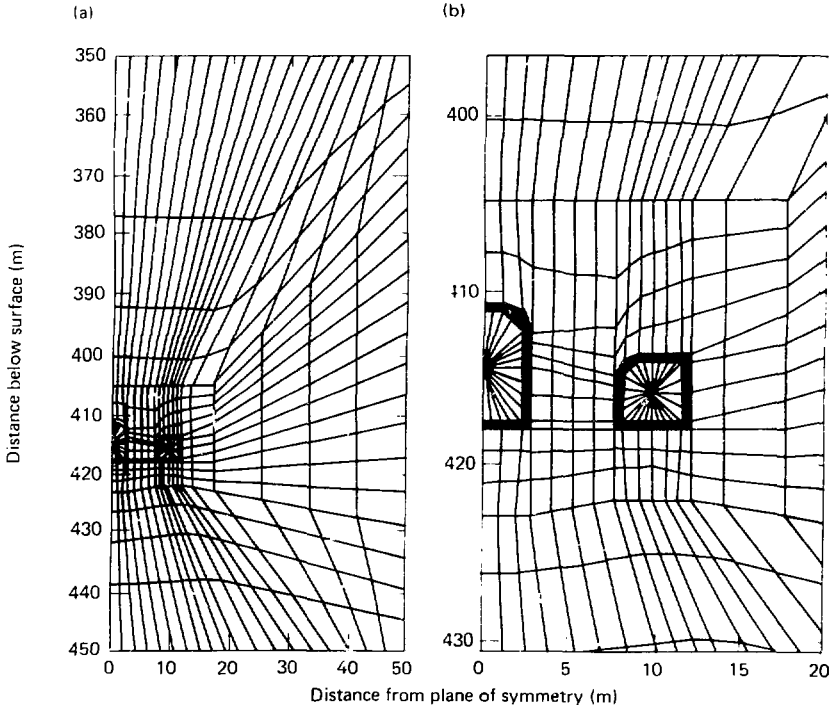

FIG. 3. Finite-element mesh used with as-built mining and thermomechanical calculations.

TABLE 2. Values of Climax Stock granite and air properties used in calculations.

A. Climax Stock granite	Values
Heat capacity[a]	930 J/kg-K
Thermal conductivity[10,11]	
0°C	3.1679 W/m-K
23°C	3.1104 W/m-K
477°C	2.1104 W/m-K
Thermal expansion coefficient[12]	
0°C	10×10^{-6} K^{-1}
23°C	10×10^{-6} K^{-1}
40	8.9×10^{-6} K^{-1}
80	7.4×10^{-6} K^{-1}
125	8.0×10^{-6} K^{-1}
175	9.6×10^{-6} K^{-1}
225	12.7×10^{-6} K^{-1}
Elastic modulus:	
Field[8]	
Explosive-damaged region	13 GPa
Rock mass	27 GPa
Laboratory[10]	
Rock samples	48 GPa
Poisson's ratio:	
Field[8]	
Rock mass	0.25
Damaged zone	0.35
Laboratory[10]	
Rock samples	0.21
B. Air[b]	
Density	1 kg/m^3
Heat capacity	1000 J/kg-K
Thermal conductivity	0.03 W/m-K

[a]Derived from diffusivity measurements.
[b]Used to derive input values shown in Table 3 (Ref. 4).

Temperature-dependent thermal-expansion coefficients are based on a suite of sample measurements taken from the spent-fuel test site.[12]

Table 3 presents drift material properties derived to simulate radiation and ventilation with ADINAT.[4]

Table 4 shows the heat input values used in the as-built calculations reported here.

Figure 4 shows the decay curves for the spent-fuel canisters. The power-level decay for the spent fuel was assumed to be proportional to that for PWR fuel, with a burnup of 33,000 megawatt days thermal per metric ton of uranium (MWD/MTU) at a specific power of 37.5 MW/MTU.[13] The electrical simulators in the canister drift were made to follow this decay curve by a series of adjustments in thermal input. Table 5 shows the power levels of the electrical resistance heaters deployed in the two parallel side drifts to simulate the thermal regime of a large repository.

TABLE 3. Values of drift material properties derived to simulate radiation and ventilation with ADINAT.

Properties	Values
Thermal conductivity:	
Spent-fuel drift	70 W/m-K
Heater drift	40 W/m-K
Volumetric heat capacity	8×10^4 J/m^3-K
Convection coefficient (H)	
ΔT (K)	H(W/m^2-K)
0	0
0.272	4.5
0.445	5.0
0.903	5.5
1.878	6.0
4.074	6.5
9.427	7.0
24.042	7.5

TABLE 4. Parameters used in as-built ADINAT heat flow calculations.

Parameters	Values
For spent-fuel canisters and electrical simulators	
Length	3.66 m (12 ft)
Power at start time	1.527 kW (decaying)[6]
Start time	May 6, 1980 (2.46 yr out of core)[a]
For electrical resistance heaters	
Length	1.83 m (6 ft)
Power at start time	1.850 kW[b]
Turn-on time	June 27, 1980 (0.14 yr since start time).

[a]Installation date of center canister.
[b]See Table 5.

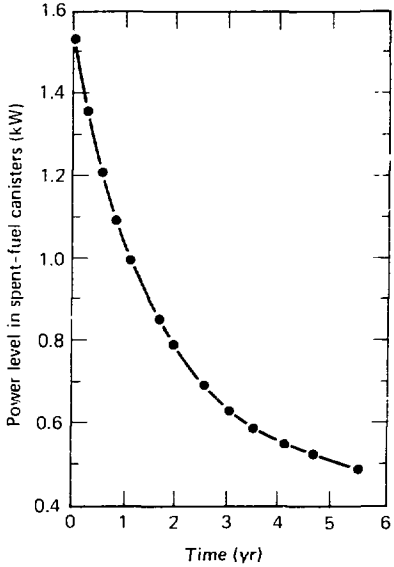

FIG. 4. Spent-fuel decay curve used in ADINAT calculations.

TABLE 5. Variation in power level in electrical-resistance heaters.

Time since emplacement (yr)	Date	Power level (kW)
0	6 May 1980	0
0.14	27 June 1980	1.850
0.16	2 July 1980	0.925
0.60	17 Dec. 1980	1.300
1.46	8 Mar. 1982	1.400

THERMAL CALCULATION

The thermal calculation was carried out with the ADINAT finite-element code, which is compatible with the ADINA displacement and stress-analysis code. ADINAT produces temperature histories that are used with the ADINA thermomechanical calculation for each node in a given finite-element mesh.

The ADINAT calculation modeled internal radiative heat transfer in the drifts by assigning the drift material a high value of thermal conductivity and low density. Ventilation was modeled with convective heat transfer from a central node in each drift. The thermal conductivity of the drift material was adjusted until the ADINAT results agreed with properly modeled TRUMP[14] code results, including radiative heat transport between drift walls, conductive and convective thermal transport to and through the air in the drifts, and mass flow of air in the drifts.[4]

Figure 5 shows the change in temperature (ΔT) contours generated during the decay of the spent-fuel below the floor of the spent-fuel drift and from the electrical resistance heaters below the floor and the heater drift. The plots are for 0.2, 0.4, 0.6, and 1.0 years since emplacement. Figure 6 shows ΔT contours at 2.0, 3.0, 4.0, and 5.0 years. The contours at 5.0 years include the ΔT = 1, 2, 3, and 4°C. Flattening of the ΔT = 1.0 contour near the outer boundary of the mesh is due to a boundary condition that fixes the temperature at ambient.

Proper modeling of radiative and convective heat transport in the drifts produces temperature contours that are asymptotic near the drift walls. If the drift voids were treated as insulators, the contours would be perpendicular

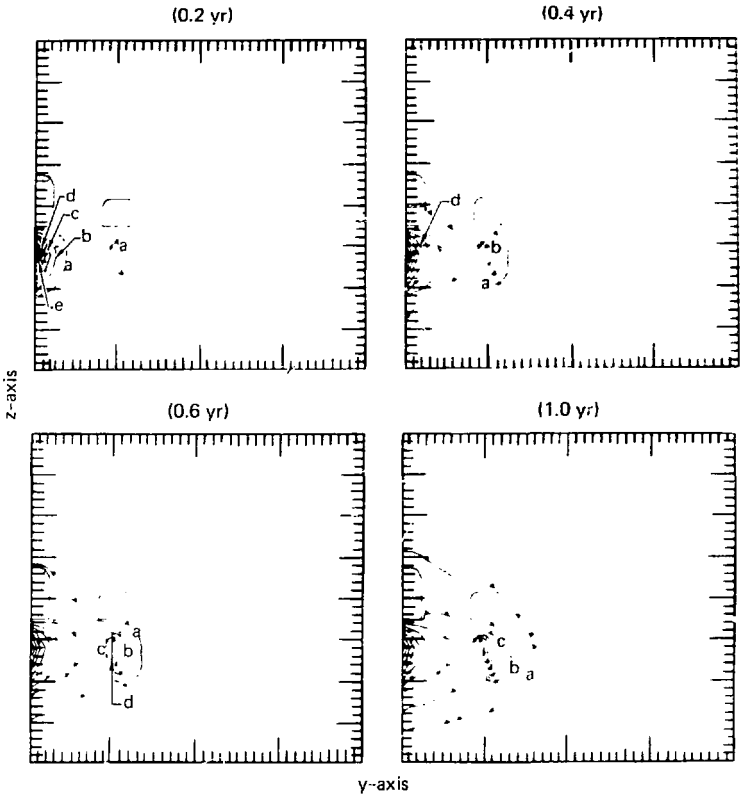

FIG. 5. ΔT contours calculated by ADINAT at different times to 1 yr from emplacement. Contour intervals in °C above ambient: B=5, C=10, D=15, E=20, F=25, G=30, H=35, I=40, J=45, K=50.

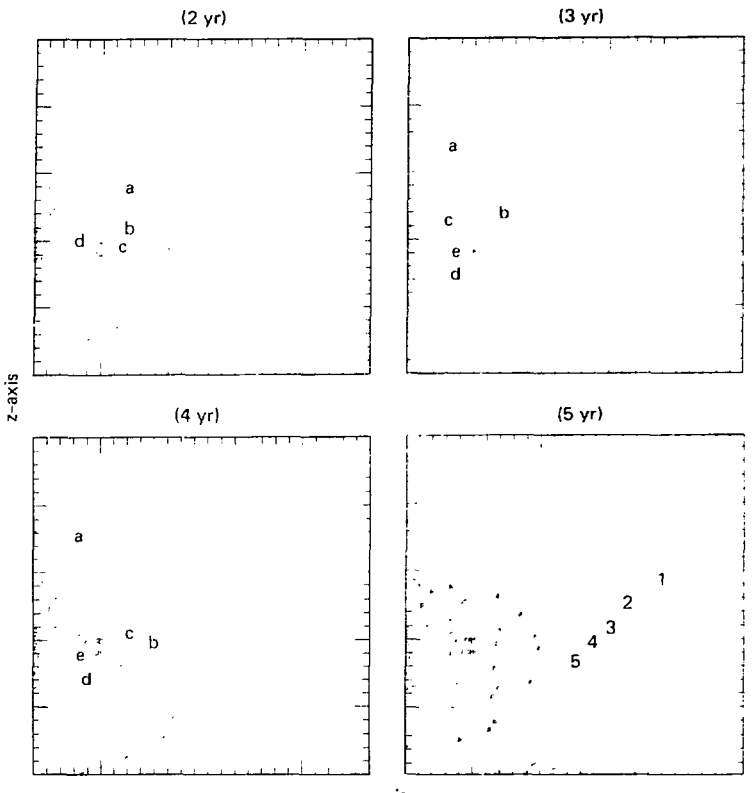

FIG. 6. ΔT contours calculated by ADINAT at different times after emplacement. Contour intervals in °C above ambient: A=5, B=10, C=15, D=20, E=25, F=30, G=35, H=40, I=45, J=50.

to the walls. Because of the radiative and convective heat transfer in the drift voids, the walls of a given drift are nearly isothermal, the drift voids being a better heat transfer medium than the excavated rock.

THERMOMECHANICAL CALCULATIONS

ADINA was run to calculate the effects of both the mining and application of the thermal load later on, and the displacements resulting from the changing stress field. The boundary conditions for the calculational mesh used roller boundaries on the axis of symmetry Y = 0, where motion is constrained in the horizontal (Y) direction; and at the lower boundary at Z = -450 m, where motion is constrained in the vertical (Z) direction. At the upper boundary, Z = -350 m, the loading of ρgh was applied in the vertical direction, where ρ is the average overburden density, g the acceleration of gravity, and h the distance below the surface. At the right boundary at Y = 50 m, the applied load increased with distance below the surface and was set equal to 1.2 ρgh. Motion is not constrained on the loaded boundaries; however, the load remains constant throughout the entire mining and thermal portion of the calculation. This loading is based on U.S. Geological Survey measurements of *in situ* stress.[9]

Heuzé and Patrick[7] show there is considerable difference between moduli values determined from field measurements and those obtained from direct measurements on laboratory samples. These authors estimate the modulus from field measurements to be around 27 GPa, while laboratory measurements give values of moduli of about 48 GPa.[10] Furthermore, an explosively damaged region with a significantly reduced modulus 0.5-0.6 m deep was found around each mined excavation.[8] Three ADINA calculations were made to study the effects of differences in moduli on the calculational results. Table 6 summarizes the input.

The first four cycles of each calculation related to the application of loads and the mining of the drifts. In Cycle 1, geostatic loads were applied. Cycles 2, 3 and 4 were for the mining portion of the calculation. In Cycle 2, the heater drifts were excavated by removing the elements in the side drifts. In practice, the spent-fuel (center) drift was excavated in two passes, the upper arched portion (heading) and then the lower portion (bench). Consequently, the heading in Cycle 3 and the bench in Cycle 4 were

TABLE 6. Elastic properties used in ADINA calculations.

Calculation	#1	#2	#3
0.5 m around openings			
Modulus	48 GPa[10]	27 GPa[8]	13 GPa[8]
Poisson's ratio	0.21	0.25	0.35
Remainder of mesh			
Modulus	48 GPa	27 GPa	27 GPa
Poisson's ratio	0.21	0.25	0.25

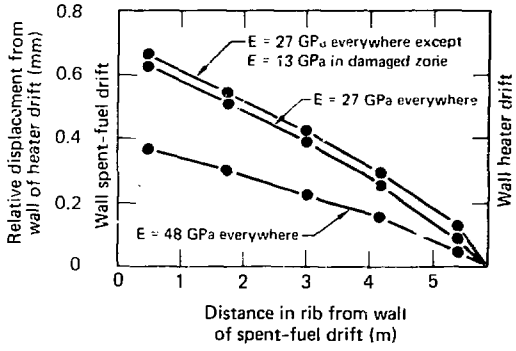

FIG. 7. Horizontal displacement in rib relative to hole collar in wall of heater drift resulting from excavation of spent-fuel drift.

excavated. The thermal portion of the calculations were run out to five years in 200 additional, equal time-step cycles.

The effect of modulus variation, as well as the explosively damaged zone around the excavations are shown in Figs. 7 and 8. As can be expected, the higher laboratory-measured modulus produces significantly smaller motions. The low modulus value in the relatively thin, damaged zone around the excavation also influences the displacements. Figure 7 shows calculated relative horizontal displacement across a pillar referenced to a hole collar at midheight in the heater drift. This resulted from mining the spent-fuel

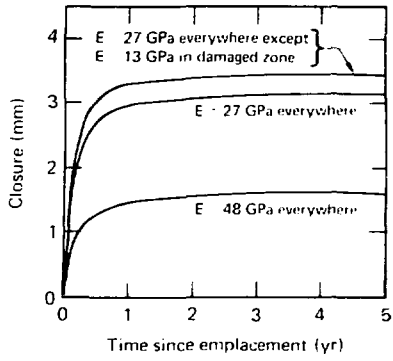

FIG. 8. Horizontal closure of spent-fuel drift from thermal load.

drift. These results show that displacements across a pillar have a nearly constant ratio equal to the ratio of the two moduli of 48 and 27 GPa. Figure 8 shows horizontal closure of the spent-fuel drift from the thermal loads as a function of time. About 50% of the maximum closure occurs during the first month after insertion of the spent-fuel and before the electrical resistance heaters were turned on. About 90% of the closure occurs within the first year. Here, the ratio of maximum closures is about 10% greater than would be obtained from the ratio of the moduli mentioned above.

The effect of various finite-element mesh loadings was also studied. Calculations of the mining phase were repeated using horizontal loadings of 0.8 and 1.0 ρgh. The sensitivity of the loading was demonstrated after selecting two nodes that lie on a line along which extensometers were installed. This line extended 34° from horizontal. Figure 9 shows the nodes with vector displacements from mining t[illegible]ent-fuel drift for three loadings. Projection of these vector displacement[illegible] the 34° extensometer give the components of displacement that would be measured by the extensometers. Note that these components of node displacements at the mid-rib are in opposite directions. Horizontal loading of 0.8 ρgh causes projection of this node down toward the heater drift, while loadings of 1.0 and 1.2 ρgh both cause projected motions upward and away from the heater drift. The motion at the wall of the heater drift is also strongly affected by the loading. For a

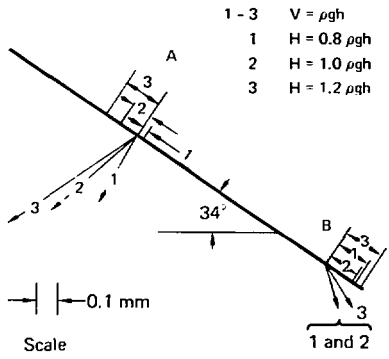

FIG. 9. Displacement of two different points in finite-element mesh from mining of spent-fuel drift. Points lie on a 34° line, along which extensometers were emplaced (cf. Fig. 2). Point A is mid-rib, point B is at heater drift wall.

point on the wall, the loading does not lead to a direction reversal since the displacements move into the heater drift void.

These calculations show that the state of *in situ* stress can strongly influence relative motion in a rock mass during the mine-by experiment. The very small vector motion of the points (0.3 to 0.5 mm) could be anything from plus or minus some fraction of this when measured by an inclined extensometer, unless emplaced in the direction of motion. The motion of the mid-rib point relative to the point on the wall of the heater drift, as measured for any of the three loadings, shows that the pillar is broadening.

The best estimates of moduli and loading were assumed to be those taken in the field. The calculation using these estimates is the one with a modulus of 27 GPa everywhere except for a 0.5-m damaged zone around each opening with a reduced modulus of 13 GPa (Calculation 3). The geostatic loading ratio of 1.20 horizontal-to-vertical stress was also obtained from field measurements. The results of this calculation are shown in more detail and should be used to compare measurements of displacement and stress as they become available from the field.

Figure 10 shows the displacement vectors of each node point from the mining phase of the calculation in the vicinity of the excavations. Figure 11

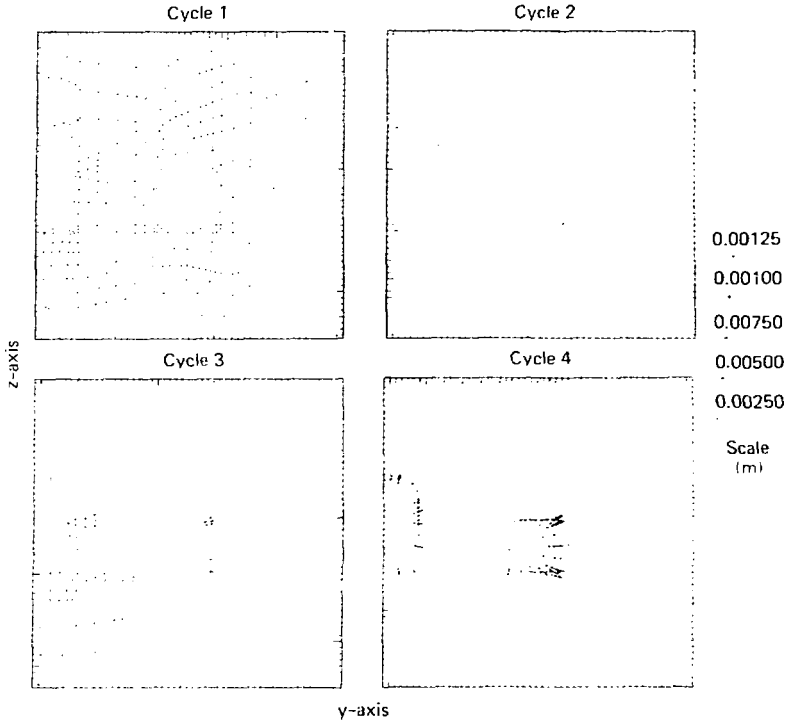

FIG. 10. Vector displacements of node points (Cycle 1) in finite-element mesh from mining heater (Cycle 2), the heading (Cycle 3), and bench (Cycle 4) of the spent-fuel drift.

shows the vector displacements of each node point in the entire mesh from mining both the heater and spent-fuel drifts. Maximum displacements are on the order of 1 mm. The displacements occur throughout the mesh, moving in the direction of openings created from mining, and including motion on those boundaries of the mesh that are free to move.

Figures 12 and 13 show displacement vectors of each node from the thermal load in the vicinity of the excavations and heat sources. Figures 14 and 15 show the displacement vectors of each node in the entire finite element mesh at various times. None of these figures include the displacements from mining, so a direct comparison with instruments installed after excavation is

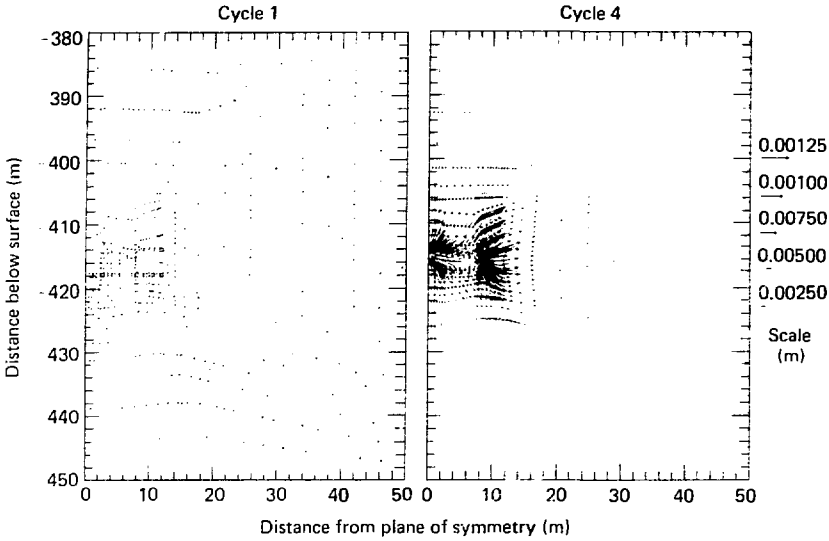

FIG. 11. Vector displacements of all node points in finite-element mesh from mining heater and spent-fuel drifts: Cycle 1 shows the mesh points before mining; Cycle 4 shows the displacements after mining.

possible. The maximum displacement during the five-year interval is of the order of 3 to 4 mm. The displacements occur throughout the mesh, with the direction of motion away from the heat sources, including outward displacements of all the boundary mesh nodes free to move.

Figure 16 shows the calculated time histories for displacement in the middle of the floor and ceiling of the spent-fuel drift from the thermal load. The ceiling is shown initially moving downward, a trend which reverses at about 0.2 years. This is probably caused by the heat-flow pattern set up by the spent-fuel line source, which also causes inward movement of the drift walls. Figure 17 represents the calculated horizontal and vertical closures of both the spent-fuel and heater drifts as a function of time. Figure 18 shows vertical displacement below the floor of the spent-fuel drift, relative to hole collars in the floor at 1.1, 1.7, and 2.1 m from the center of the drift, i.e., as a function of distance below the floor at 0.5 and 1.2 years.

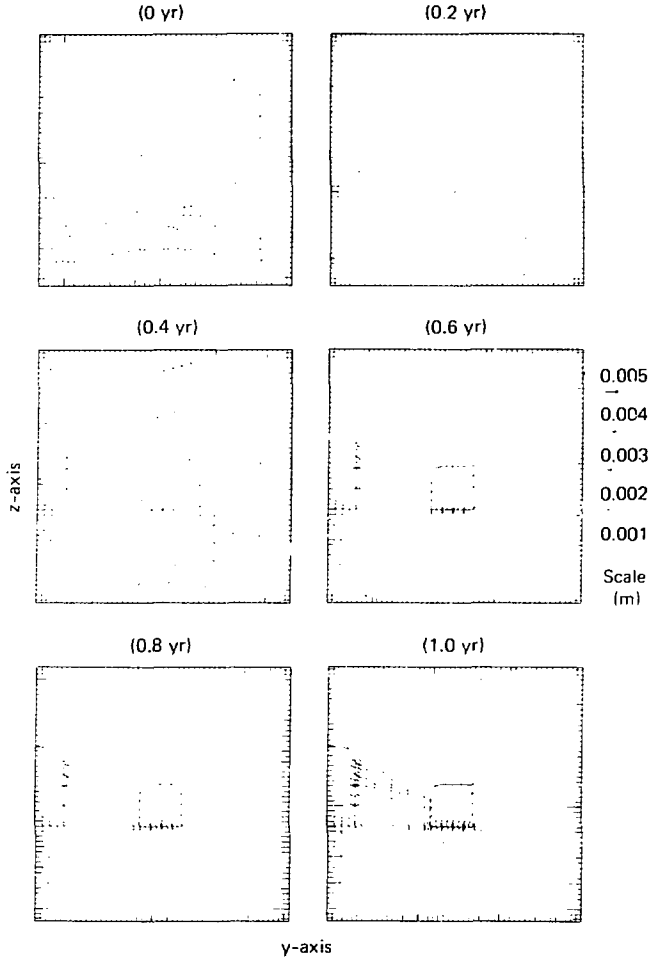

FIG. 12. Vector displacements of nodal points in finite-element mesh as a result of the thermal load: at 0, 0.2, 0.4, 0.6, 0.8, and 1.0 yr since emplacement. Rock modulus = 27 GPa, damaged rock modulus = 13 GPa.

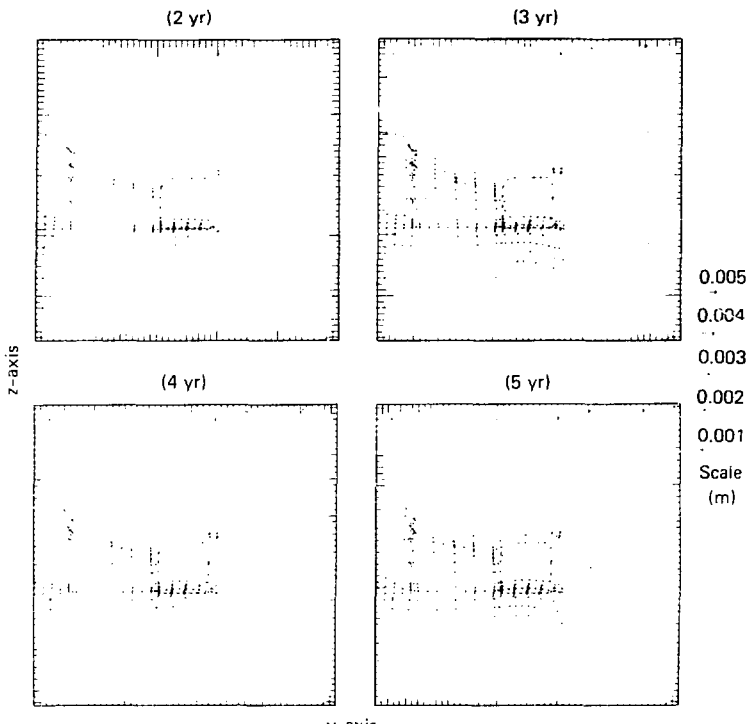

FIG. 13. Vector displacements of nodal points due to thermal load at 2.0, 3.0, 4.0, and 5.0 yr after emplacement. Rock modulus = 27 GPa, damaged rock modulus = 13 GPa.

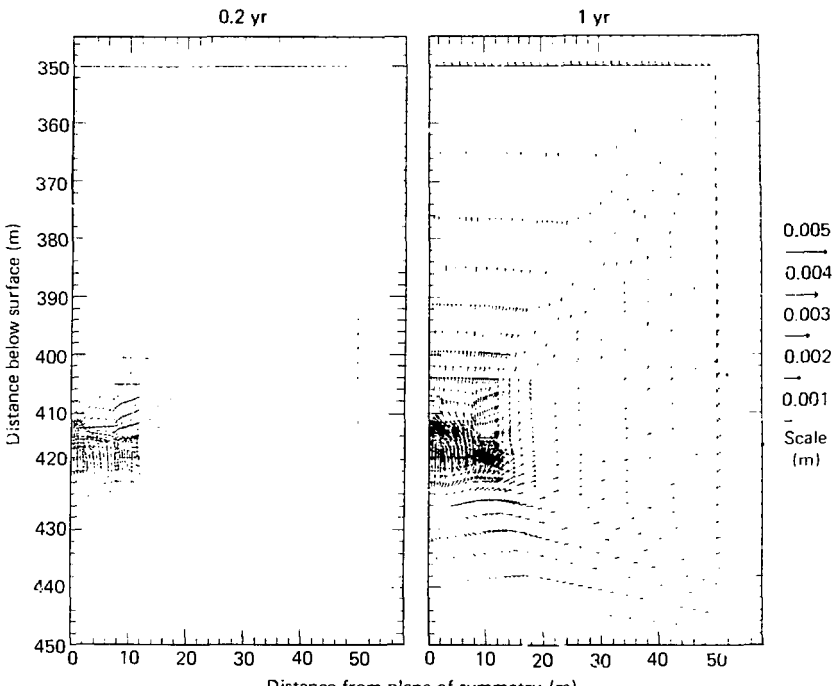

FIG. 14. Vector displacements of nodal points in the entire mesh due to thermal load at 2 and 5 yr after emplacement. Rock modulus = 27 GPa, damaged rock modulus = 13 GPa.

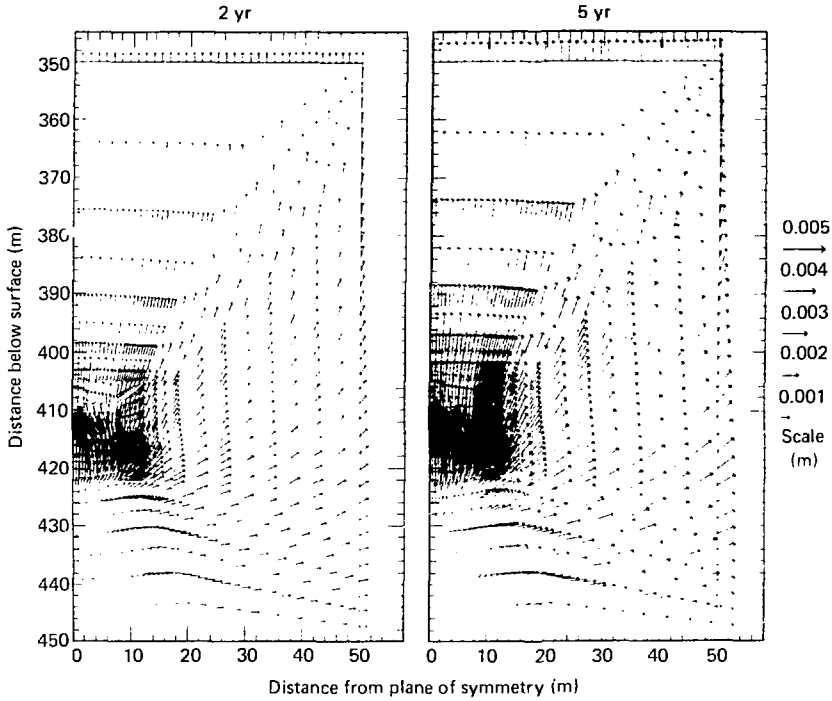

FIG. 15. Vector displacements of nodal points in the entire mesh due to thermal load at 0.2 and 1 yr after emplacement. Rock modulus = 27 GPa, damaged rock modulus = 13 GPa.

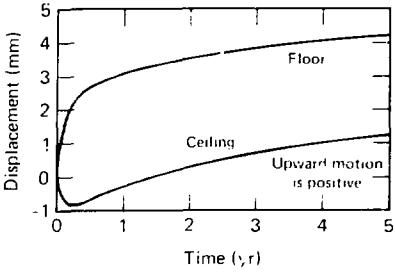

FIG. 16. Vertical displacement at centerline of spent-fuel drift from thermal load. ADINA calculation with damaged rock.

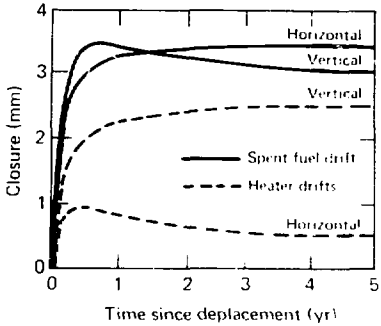

FIG. 17. Closure of spent-fuel and heater drifts from thermal load. ADINA calculation with damaged rock.

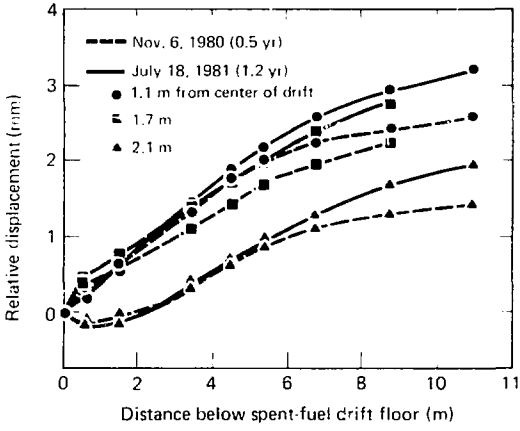

FIG. 18. Relative vertical displacements below floor of spent-fuel drift to hole collars at different distances from center of drift. Modulus = 27 GPa except in damaged rock.

The stress contours in Figs. 19 through 22 were plotted as reflected about the plane of symmetry passing midway through the central drift. The shapes of the contour are caused by the heat sources below the drifts and are also due to the drift walls being heat sources. This is caused from the radiative heat flow across the drifts, making the openings better heat conductors than the surrounding rock. Horizontal and vertical tensile stresses are calculated only for those elements in the damaged zone that form the lower corners between the floor and wall of the spent-fuel and heater drifts. These areas are near the heat sources and also near where the high, radiative heat flow through the drifts and relatively low heat flow through the rock mass merge. The highly-jointed rock mass in Climax Stock granite, including the damaged region around the openings, undoubtedly has some effective tensile strength, but it is not required for the integrity of the underground openings. The results calculated used the ADINA code's thermoelastic model (which models the rock mass to be homogeneous and isotropic and has no failure model). It is doubtful that a tensile stress as large as 3 MPa would actually develop in a highly-jointed rock.

Figures 23 to 25 show stress-vs-time plots at locations where vibrating-wire stress gauges were installed. The first four points on each figure are for the loading and excavation phases of the calculations. Figure 23 is a location midheight on a spent-fuel canister, 1.18 m from its axis. Figure 24 shows a location at pillar midheight, 0.7 m in from the spent-fuel drift. Figure 25 shows a location at pillar midheight, 3 m in from the heater drift. The stresses introduced from geostatic loading are changed only slightly as a result of the excavations in the vicinity of the spent-fuel canister. Both the vertical and horizontal stresses reach their maximum value within one year after heating starts and they slowly decrease as the spent-fuel decays. At the locations in the pillars, the vertical stress increases and the horizontal stress decreases during the excavation phase, and continue to do so during the thermal input phase, reaching their respective maximum and minimum in the first 0.5 years. In both of the pillar locations the horizontal stresses are only slightly compressive after this time.

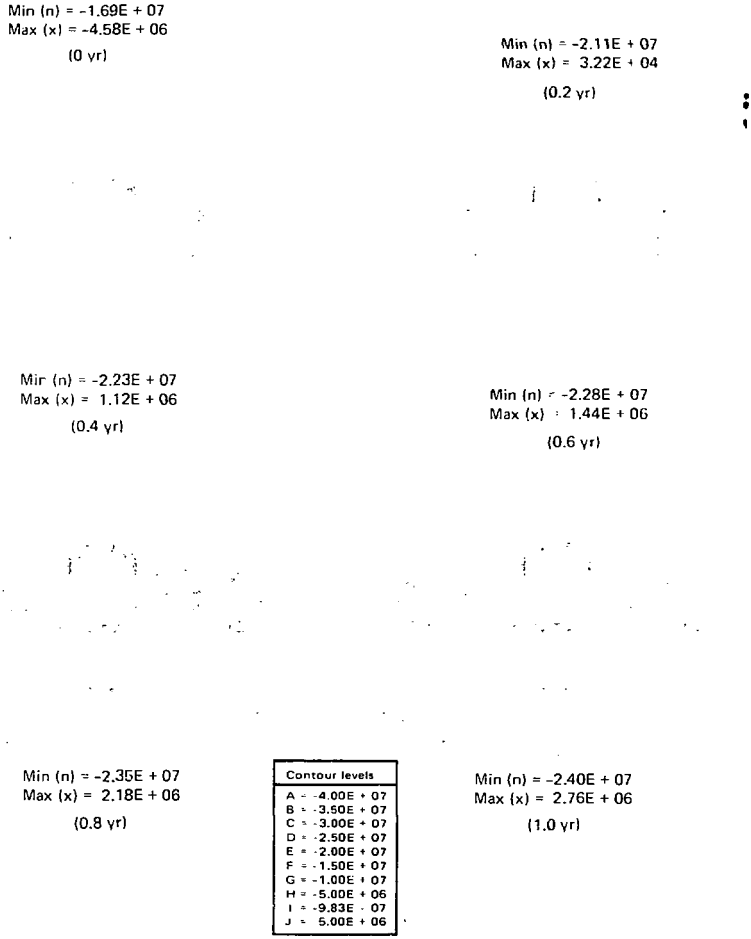

FIG. 19. Horizontal (Y) stress contours around excavations at various times after emplacement of spent-fuel canisters. Rock modulus = 27 GPa except in damaged rock = 13 GPa. Stress units are pascals.

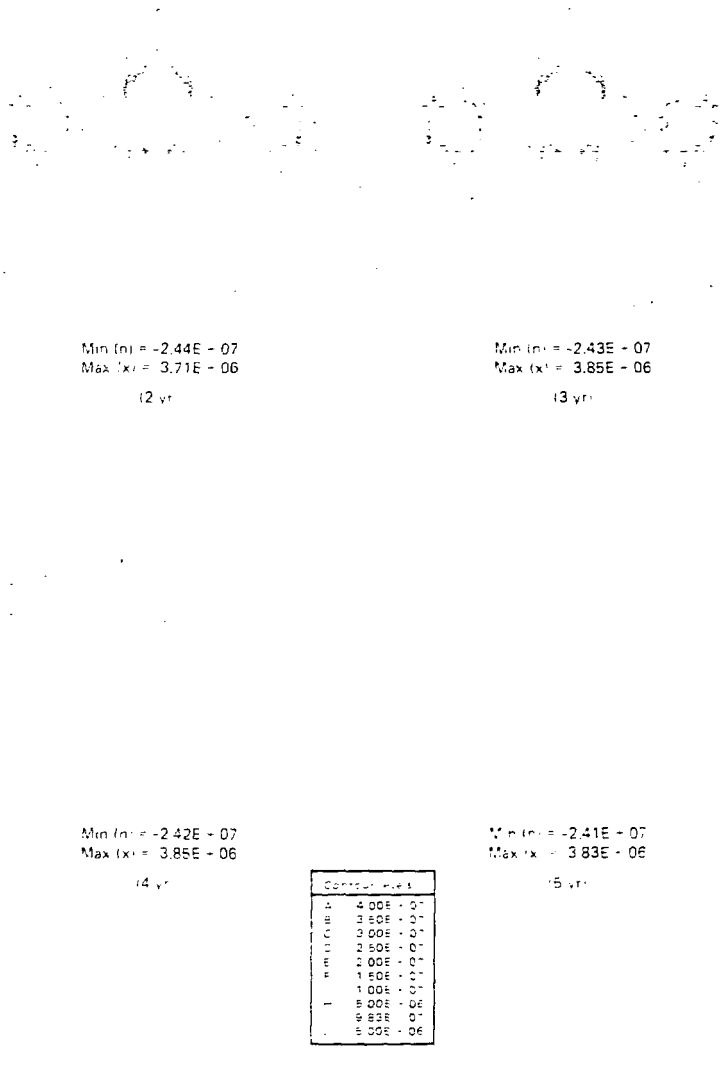

FIG. 20. Horizontal (Y) stress contours around excavations at various times after emplacement of spent-fuel canisters. Rock modulus = 27 GPa except in damaged rock = 13 GPa. Stress units are pascals.

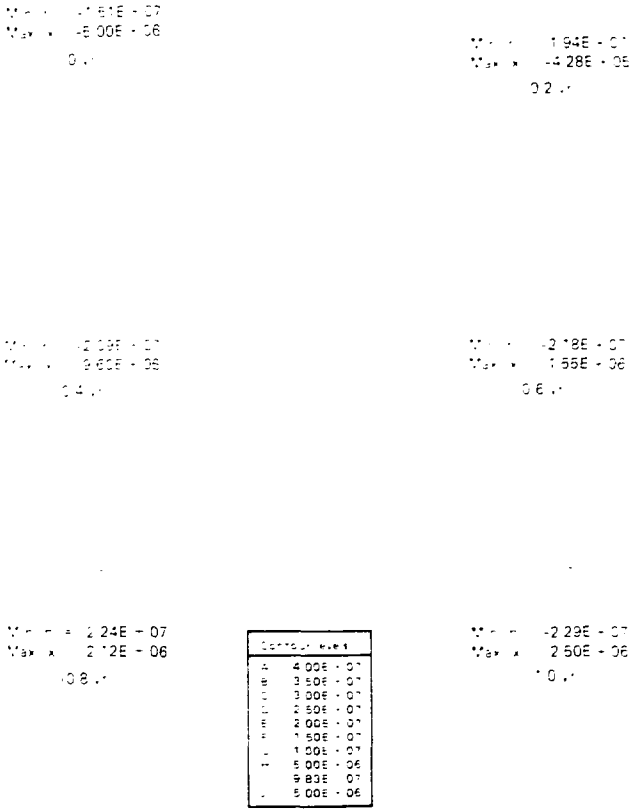

FIG. 21. Vertical (Z) stress contours around excavations at various times after emplacement of spent-fuel canisters. Rock modulus = 27 GPa except in damaged rock = 13 GPa. Stress units are pascals.

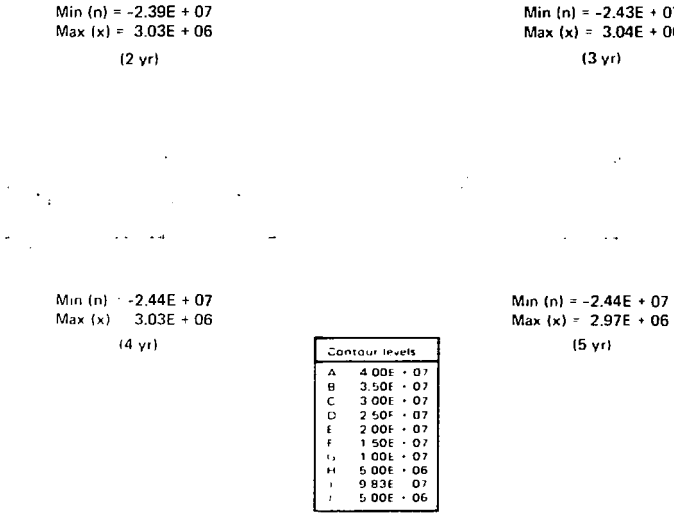

FIG. 22. Vertical stress contours around excavations at various times after emplacement of spent-fuel canisters. Rock modulus = 27 GPa except in damaged rock = 13 GPa. Stress units are pascals.

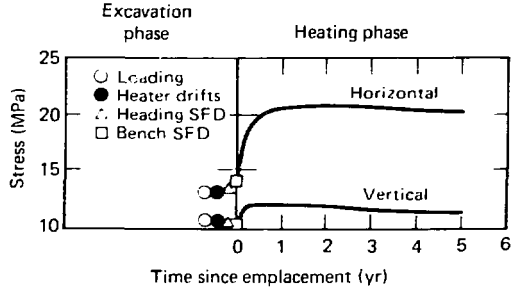

FIG. 23. ADINA as-built calculation with damaged rock stress vs time at the midpoint elevation of a spent-fuel canister, 1.18 m from its axis.

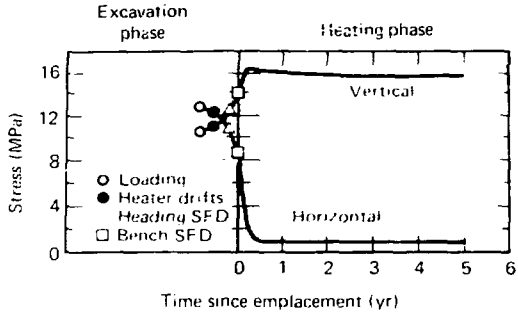

FIG. 24. ADINA as-built calculation with damaged rock stress vs time at a point midheight of rib, 0.7 m from spent-fuel drift.

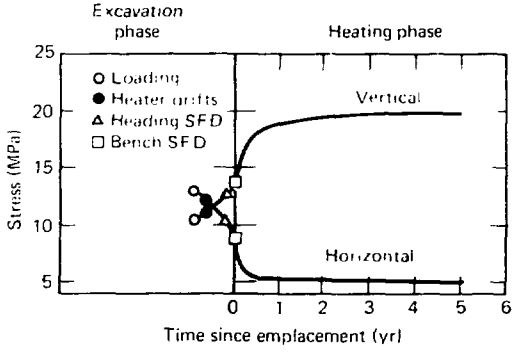

FIG. 25. ADINA as-built calculation with damaged rock stress vs time at a point midheight of rib, 3 m from heater drift.

SUMMARY AND RESULTS

The preemplacement calculations that were made using the ADINA stress code and the compatible ADINAT heat-flow code were intended to provide a base with which to compare temperature, stress, and displacement data taken during the planned 3- to 5-year duration of the test. Through such a comparison it would be possible to determine how the existing jointing in the Climax Stock

granite influenced the results as compared with a homogeneous isotropic rock mass assumed in the calculations. Since then, several determinations have been made that can have significant effects on the calculational results.

1. Calorimetric measurements of the spent-fuel element showed that the expected heat output was about 22% too high. Because of this, the planned power levels of the electrical simulators and auxiliary heaters were changed.

2. *In situ* field measurements of the effective modulus of the Climax Stock granite were made. These showed that the *in situ* modulus is about a factor of two less than laboratory measurements on samples taken from the site.

3. *In situ* field measurements also show an explosively-damaged region around each excavation with a modulus of about a factor of two below that of the surrounding rock.

4. Field measurements of *in situ* stress show that the ratio of horizontal-to-vertical stress can be as high as 1.25.

The calculational results reported here were made with up-to-date knowledge of thermal loading, including changes already made or planned changes in the output of the electrical resistance sources in the heater drift floor. The thermal properties of the rock mass are based on both pressure- and temperature-dependent expansion coefficient measured on samples in the laboratory, and laboratory and field measurements of thermal conductivity.

In the ADINA structural analysis calculations, we studied the sensitivity of the modulus used, the effect of including an explosively-damaged zone, and how the loading affected the calculated displacements and stresses. As might be expected, these studies show the importance of accurately determining *in situ* stress and effective moduli. Displacements and stresses were found to be proportional to the effective modulus used and, when including a small explosively damaged region around the excavation, can increase the displacements by as much as 10%. The ratio of horizontal-to-vertical loading stress was also found to be important, particularly when considering measurement of relative displacements at some azimuth off horizontal. Changing the loading ratio from 0.8 to 1.0 ρgh reverses the projected direction of motion of an anchor point on the 34° extensometer in the example shown.

These thermomechanical calculations with the ADINA code used input parameters of moduli and loading that are deemed the best estimates for these quantities. Best-estimate properties include an explosively-damaged region around the mined openings with a modulus of 13 GPa. Elsewhere the modulus was

27 GPa.[7] The *in situ* stress field used a ratio of horizontal-to-vertical stress of 1.2, based on USGS measurements.[9]

The calculations presented in this report use best-estimate values of rock properties and *in situ* stress and are not intended to predict the motions and stress changes from mining and thermal load. Existing jointing in the Climax Stock granite could have a significant effect on the actual displacements and stress field. Such effects are not accounted for in the calculations reported here. However, these calculations do indicate the extent and magnitude of motion and stresses that would be expected in the absence of jointing. Comparison of these results with actual field measurements will then indicate whether a joint model should be included in future calculations.

The calculations described here are in a quality assurance project archive. The archive contains microfiche records of input and output files generated to obtain the results reported here. These calculations were completed between March and April 1981 without consideration of available stress and displacement data.

ACKNOWLEDGMENTS

John Peterson installed the ADINA and ADINAT codes on the CRAY computer, which made the calculations much easier to run than with the system previously used. In addition, John greatly improved the post-processing package, which facilitated temperature contour plotting and added the new capability of vector displacement plots.

François Heuzé, who did the field measurement of *in situ* moduli, suggested the best estimate of the modulus and loading used in the calculations.

Wesley Patrick critically reviewed this report and offered several useful suggestions.

REFERENCES

1. Butkovich, T. R., *Mechanical and Thermomechanical Calculations Related to the Storage of Spent Nuclear Fuel Assemblies in Granite*, Lawrence Livermore National Laboratory, Livermore, Calif., UCRL-52985 (1980).
2. Bathe, K. J., *ADINA, a Finite Element Program for Automatic Dynamic Incremental Nonlinear Analysis*, Massachusetts Institute of Technology, Cambridge, Mass., 82448-1 (1978).
3. Bathe, K. J., *ADINAT, a Finite Element Program for Automatic Dynamic Incremental Analysis of Temperature*, Massachusetts Institute of Technology, Cambridge, Mass., 82448-5 (1977).
4. Butkovich, T. R., and D. N. Montan, *A Method for Calculating Internal Radiation and Ventilation with the ADINAT Heat Flow Code*, Lawrence Livermore National Laboratory, Livermore, Calif., UCRL-52918 (1980).
5. Bell, M. J., *ORIGEN, the ORNL Isotope Generation and Depletion Code*, Oak Ridge National Laboratory, Oak Ridge, Tenn., ORNL-4628 (1973).
6. Schmittroth, F., G. J. Neeley, and J. C. Krogness, *A Comparison of Calculated Decay Heat for Spent Fuel Near 2.5 Years Cooling Time*, Hanford Engineering Development Laboratory, Richland, Washington, HEDL-TC-1759 (1980). (Preliminary-controlled distribution.)
7. Heuzé, F., W. Patrick, R. De La Cruz, and R. Voss, *In Situ Deformability, In Situ Stresses, and In Situ Poisson's Ratio, Climax Granite, Nevada Test Site*, Lawrence Livermore National Laboratory, Livermore, Calif., UCRL-53076 (1980).
8. Heuzé, F. E., T. R. Butkovich, and J. C. Peterson, *An Analysis of the Mine-By Experiment, Climax Granite, Nevada Test Site*, Lawrence Livermore National Laboratory, Livermore, Calif., UCRL-85622 (1981).
9. Ellis, W. L., and J. E. Wagner, *Determination of In Situ Stress in Spent-Fuel Test Facility*, Climax Stock, Nevada Test Site, USGS Denver (in preparation).
10. Pratt, H., R. Lingle, and T. Schrauf, *Laboratory Measured Material Properties of Quartz Monzonite, Climax Stock, Nevada Test Site*, Lawrence Livermore National Laboratory, Livermore, Calif., UCRL-15073 (1979).
11. Bradkin, W., and D. Montan, *Final Report, Heater Test #1*, Lawrence Livermore National Laboratory, Livermore, Calif. (in preparation).

12. Heard, H. C., *Thermal Expansion and Inferred Permeability of Climax Quartz Monzonite to 300°C and 27.6 MPa*, Lawrence Livermore National Laboratory, Livermore, Calif., UCRL-83697 (1979).

13. *Spent Unreprocessed Fuel Facility Engineering Studies*, Rockwell International Corporation, Hanford, Washington, Informal Report RHO-LD-2 (1978).

14. Edwards, A. L., *TRUMP, a Computer Program for Transient and Steady State Temperature Distribution in Multi-Dimensional Systems*, Lawrence Livermore National Laboratory, Livermore, Calif., UCRL-14754. Rev. 3 (1972).